miR663a-TTC22V1 axis inhibits colon cancer metastasis

WEI TIAN*, YANTAO DU*, YUWAN MA*, BAOZHEN ZHANG, LIANKUN GU, JING ZHOU and DAJUN DENG

Key Laboratory of Carcinogenesis and Translational Research (Ministry of Education/Beijing), Division of Etiology, Peking University Cancer Hospital and Institute, Beijing 100142, P.R. China

Received May 4, 2018; Accepted January 10, 2019

DOI: 10.3892/or.2019.6969

Abstract. An increasing number of studies have demonstrated that microRNAs (miRs) may act as oncogenes or anti-oncogenes in various types of cancer, including colon cancer (CC). However, the clinical and biological significance of *miR663a* in the prognosis of CC and its underlying molecular mechanisms remain unknown. Using the reverse transcription-quantitative polymerase chain reaction on CC and surgical margin tissue samples from 172 patients with CC, it was identified that *miR663a* was significantly downregulated in CC (P<0.001), particularly in metastatic CC (P=0.044). *miR663a* overexpression inhibited the proliferation and migration/invasion of CC cells *in vitro*, and also tumor growth and metastasis of CC cells *in vivo*. Additionally, *miR663a* target genes were analyzed. Inverse changes in tetratricopeptide repeat domain 22 variant 1 (*TTC22V1*) in response to alterations in *miR663a* expression were observed. *miR663a* decreased the reporter activity of the wild-type *TTC22V1*-3' untranslated region (UTR), but did not decrease that of a 3'UTR mutant. *miR663a* completely abolished cell migration/invasion induced by *TTC22V1* containing the wild-type 3'UTR sequence, but not that induced by *TTC22V1* containing the 3'UTR mutant. An inverse correlation between *miR663a* and *TTC22* mRNA levels was observed in CC tissues. These results suggest that *TTC22V1* mRNA is a crucial *miR663a* target that directly promotes cell migration/invasion. TTC22, which, to the best of our knowledge, has rarely been investigated, is located in the nuclei of epithelial cells in colon stem cell niches at crypt bases, and is significantly downregulated in CC, particularly in non-metastatic CC. High *TTC22V1* expression is a significant poor survival factor for patients with CC. Collectively, the results of the present study suggested that *TTC22V1* may be a metastasis-associated gene and that the *miR663a-TTC22V1* axis inhibited CC metastasis.

Correspondence to: Professor Dajun Deng, Key Laboratory of Carcinogenesis and Translational Research (Ministry of Education/Beijing), Division of Etiology, Peking University Cancer Hospital and Institute, 52 Fu-Cheng-Lu, Beijing 100142, P.R. China
E-mail: dengdajun@bjmu.edu.cn

*Contributed equally

Abbreviations: CC, colon cancer; *TTC22V1*, tetratricopeptide repeat domain 22 variant 1; SM, surgical margin; UTR, untranslated region; 3'UTR-wt, wild-type *TTC22V1* 3'UTR; 3'UTR-mut, 3'UTR-mutant control; *TTC22V1*&3'UTR-wt, *TTC22V1* cDNA sequence containing a wild-type 3'UTR; *TTC22V1*&3'UTR-mut, *TTC22V1* cDNA sequence containing a 3'UTR mutant

Key words: microRNA-663a, tetratricopeptide repeat domain 22 variant 1, colon cancer, metastasis, overall survival time

Introduction

Primate-specific microRNA-663a (*miR663a*) is associated with a number of biological processes, including viral infection and autoimmune diseases, particularly inflammation (1-6). Inflammation contributes to cancer development and progression. However, the effects of *miR663a* on cancer development remain poorly understood. The reported roles of *miR663a* in cancer development and progression are contradictory. Whereas *miR663a* may promote malignancy in prostate and nasopharyngeal cancers (7-9), it may also suppress brain and pancreatic cancers (10-12), suggesting organ-specific roles for *miR663a* in cancer development. We recently identified that metastasis-associated lung adenocarcinoma transcript 1, a competing endogenous RNA, is a master regulator of *miR663a* through a direct microRNA (miRNA)-long non-coding RNA interaction (13). A number of *miR663a* target genes (e.g. *APC*, *CDKN2A*, *CXCR4*, *eEF1A2*, *HMGA2*, *JUND*, *CDKN1A* and *TGFB1*) have been reported in various cell lineages (4,7-16); however, whether the expression patterns of these target genes contribute to the organ-specific roles of *miR663a* in cancer development remains unclear.

Tetratricopeptide repeat (TPR) domain 22 (*TTC22*) is a gene that has rarely been investigated (17). TPR motifs are present in a variety of proteins. The majority of TPR motifs are associated with multi-protein complexes. There is extensive evidence indicating that TPR motifs are important for functions associated with the cell cycle, transcription, protein transport complexes and other protein-protein interactions (18,19). According to the Human Protein Atlas (20), the *TTC22* gene is expressed comprehensively in epithelial cells in the normal gastrointestinal tract mucosa, but is lacking in gastrointestinal cancer tissues, suggesting a possible role for *TTC22* in the development and progression of colon cancer (CC).

Bioinformatics analysis results indicated that *TTC22* variant 1 (*TTC22V1*) mRNA may be an *miR663a* candidate target. In the present study, alterations in *miR663a* and *TTC22V1* expression during CC development and their association with CC progression were investigated. Most importantly, for the first time, to the best of our knowledge, *TTC22V1* is identified as a key *miR663a* target and that the *miR663a-TTC22V1* axis serves a crucial role in promoting CC metastasis.

Materials and methods

Patients and tissue samples. CC and paired non-cancerous surgical margin (SM; >5 cm from the cancer mass) samples were collected from 172 inpatients (average age, 61.6 years; 101 males and 71 females; 89 patients with CC at pathological tumor-node-metastasis stage I-II (21) and 83 patients with CC at stage III-IV) beTween-2004 and 2011 at the Biological Sample Bank, Peking University Cancer Hospital and Institute, Beijing, China (Table I). Clinicopathological and 3-year follow-up data were available for all patients.

RNA extraction and reverse transcription-quantitative polymerase chain reaction (RT-qPCR). In total, 50 ng RNA was extracted from fresh tissue samples or cell lines using TRIzol® reagent (Thermo Fisher Scientific, Inc., Waltham, MA, USA), according to the manufacturer's protocol (25˚C for 10 min and 42˚C for 30 min). The quality and concentration of the RNA samples were determined using a NanoDrop 2000 system (Thermo Fisher Scientific, Inc.). The amount of mature *miR663a* (Entrez Gene accession no. 724033) transcripts was determined using a Bulge-Loop™ miRNA RT-qPCR starter kit (cat. no. 10211; Guangzhou RiboBio Co., Ltd., Guangzhou, China) and a Bulge-Loop hsa-miR-663a RT-qPCR primer set (miRQ0003326-1; Guangzhou RiboBio Co., Ltd.), according to the manufacturer's protocol. *U6* RNA was used as a RT-qPCR reference. The thermocycling conditions were 40 cycles of 95˚C for 2 sec, 62˚C for 20 sec and 72˚C for 30 sec for *miR663a* and *U6*. *TTC22V1* (Entrez gene accession no. 55001) expression was determined using a StepOne Real-Time PCR system (Applied Biosystems; Thermo Fisher Scientific, Inc.) and SYBR-Green PCR master mix reagent (FastStart Universal SYBR-Green Master; Roche Diagnostics GmbH, Mannheim, Germany), according to the manufacturer's protocol with forward primer, 5'-atccacatcagagcctacctg-3' and reverse primer, 5'-cgtccacgcccatatagtagt-3'. Gene expression levels were normalized to those of *GAPDH* (forward primer, 5'-gaaggtgaaggtcggagt-3' and reverse primer, 5'-gaggatg-gtgatgggatttc-3') or to those of *ALU* (forward primer, 5'-gaggctgaggcaggagaatcg-3' and reverse primer, 5'-gtcgcccag-gctggagtg-3') as in the previous correlation analysis (22). The thermocycling conditions were 40 cycles of 95˚C for 15 sec, 58˚C for 20 sec and 72˚C for 30 sec for *TTC22V1*, *GAPDH* and *ALU*. Relative mRNA levels were calculated using the ΔΔCq method (23). Each sample was evaluated in triplicate.

Cell lines, culture and authentication. The HCT116 and SW480 cancer cell lines were purchased from the American Type Culture Collection (Manassas, VA, USA). The RKO cell line was kindly provided by Dr Guoren Deng (University of California San Francisco, San Francisco, CA, USA). The cell lines were cultured in RPMI-1640 medium containing 10% fetal bovine serum (FBS) and 100 U/ml penicillin/streptomycin (Thermo Fisher Scientific, Inc.) at 37˚C in a humidified incubator containing 5% CO_2. The Caco2 cell line was purchased from the National Infrastructure of Cell Line Resource (Beijing, China), and was cultured in minimal essential medium containing 10% FBS and 1% non-essential amino acids (Thermo Fisher Scientific, Inc.). All cell lines were tested and authenticated using the Goldeneye20A STR Identifiler PCR Amplification kit (Beijing Jianlian Genes Technology Co., Ltd., Beijing, China) prior to use in the study.

Plasmids, oligonucleotides and transfection. *miR663a* mimic (forward, 5'-aggcggggcgccgcgggaccgc-3' and reverse, 5'-ggucccgcggcgccccgccuuu-3'); and antisense/inhibitor (5'-gcggucccgcggcgccccgccu-3') products were synthesized by Shanghai GenePharma Co., Ltd. (Shanghai, China). A scrambled short interfering RNA set (dsR-Ctrl; forward, 5'-uucuccgaacgugucacgutt-3' and reverse, 5'-acgugacacguucg-gagaatt-3') was used as the mimic negative control. A scrambled RNA (ssR-Ctrl; 5'-caguacuuuuguguaguacaa-3') was used as the inhibitor negative control (13).

An *miR663a* expression vector, pcDNA3.1b_pri-miR663a, was constructed with 93-bp PCR products (95˚C for 30 sec, 54˚C for 30 sec, and 72˚C for 50 sec for 35 cycles) amplified from A549 cell genomic DNA using HiFi DNA polymerase, forward primer, 5'-ccttccggcgtcccaggcg-3' and reverse primer, 5'-catggccgggccaccaggaaa-3'. Green fluorescent protein (GFP)-tagged *miR663a* (GFP-*miR663a*, 5'-aggcggggcgccgc-gggaccgc-3') expression vectors were purchased from Shanghai GenePharma Co., Ltd. for stable transfection. A scrambled RNA (5'-aaatgtactgcgcgtggagac-3') expression vector was used as a negative control (13).

The wild-type *TTC22V1* 3' untranslated region (UTR) (3'UTR-wt) plasmid was cloned from A549 cells using forward primer, 5'-gatctctagagtgcggctgctcttcgagaccat-3' and reverse primer, 5-atgctctagagtcacaattcccgaccaagaatcgaa-3'. The 3'UTR-mutant control (3'UTR-mut) plasmid was constructed using a site mutation kit (Agilent Technologies, Inc., Santa Clara, CA, USA). A *TTC22V1* expression vector, pCMV6-Entry_TTC22V1, was purchased from OriGene Technologies, Inc. (cat. no. RC225966; Rockville, MD, USA). Wild-type and mutant 3'UTR sequences were synthesized and inserted into the 3'-terminus of the *TTC22V1* DNA sequence in the expression vectors (*TTC22V1*&3'UTR-wt and *TTC22V1*&3'UTR-mut, respectively) to investigate the contribution of *TTC22V1* to the inhibition of CC development by *miR663a*.

The plasmids or oligonucleotides (final concentration, 1 μg/ml) were transfected using X-tremeGENE™ HP DNA transfection reagent (Roche Diagnostics GmbH). At 24 h post-transfection, the medium was replaced with RPMI-1640 containing 10% FBS. The entire process was performed according to the manufacturer's protocol.

Western blotting. Western blotting was performed as previously described (24). Briefly, HCT116, RKO and MKN45 cells ($1.5x10^6$) were harvested at 500 x g for 5 min. Proteins

were extracted and diluted in 200 μl 1X cell lysis buffer [50 mmol/l Tris/HCl (pH 6.8), 100 mmol/l DTT, 2% SDS, 0.1% bromophenol blue and 10% glycerol] and 20 μl protein lysate was loaded per lane. Proteins were separated by SDS-PAGE (10% gel). The following primary antibodies were used: Goat anti-TTC22 polyclonal antibody (4˚C; 1:1,000; cat. no. sc-249130; Santa Cruz Biotechnology, Inc., Dallas, TX, USA), and mouse anti-GAPDH monoclonal antibody (4˚C; 1:10,000; cat. no. 97166; Cell Signaling Technology, Inc., Danvers, MA, USA). The horseradish peroxidase-conjugated anti-mouse or -goat secondary antibody (cat. no. ZB-2306 or ZB-2305; ZhongShan Jinqiao Biotechnology, Co., Ltd. Beijing, China) was incubated at room temperature for 45 min at a dilution of 1:2,000 in 1% fat-free milk. For tissue samples, proteins from 50 mg tissue were extracted and diluted in 500 μl 1X cell lysis buffer. Other processes were the same as for cell samples.

Immunohistochemistry staining (IHC). A rabbit anti-TTC22 polyclonal antibody (1:500; cat. no. HPA035072, specific for TTC22V1; Sigma-Aldrich; Merck KGaA, Darmstadt, Germany) was used for the IHC analysis. The Dako REAL™ EnVision™ Detection system (peroxidase/diaminobenzidine+, rabbit/mouse; Dako; Agilent Technologies, Inc.) was used to visualize the primary antibody-binding cells according to the manufacturer's protocol. Briefly, paraffin sections (4 μm) were dewaxed and rehydrated in xylene and ethanol. The sections were autoclaved in a 10 mM sodium citrate buffer containing 0.05% Tween-20 (pH 6.0) for 3 min for antigen retrieval and then immersed in 3% H_2O_2 for 10 min to block endogenous peroxidase. Following submerging in 5% bovine serum albumin (BSA) (cat. no. A1933; Sigma Life Science; Merck KGaA) for 60 min, the sections were incubated with the primary antibody overnight at 4˚C. The PBS-washed sections were then treated with the Dako REAL™ EnVision™ Detection system and counterstained with hematoxylin (0.125%; ZhongShan Jinqiao Biotechnology, Co., Ltd.) at room temperature for 1 min. Normal rabbit IgG (cat. no. ZDR-5118; ZhongShan Jinqiao Biotechnology, Co., Ltd.) was used as the negative control (diluted and incubated as for the anti-TTC22 antibody).

Confocal microscopic determination of TTC22V1 protein expression. TTC22V1 protein expression in Caco2, HCT116 and SW480 cells was analyzed using the aforementioned rabbit anti-TTC22 polyclonal antibody. The rabbit IgG antibody was used as a negative control. Briefly, HCT116, SW480 and Caco2 cells were cultured on coverslips and fixed with 10% paraformaldehyde for 10 min at room temperature, followed by permeabilization with 0.5% Triton X-100 in PBS for 15 min and blocking with 5% BSA overnight at 4˚C. Following incubation with the anti-TTC22V1 antibody (1:500) or the rabbit IgG negative control antibody for 2 h at room temperature, the cells were probed with a fluorescein isothiocyanate-conjugated secondary antibody (1:100 in PBS at room temperature for 45 min; cat. no. ZF-0311; ZhongShan Jinqiao Biotechnology, Co., Ltd.), counterstained with DAPI (1 μg/ml) at room temperature for 10 min, and mounted with 50% glycerol in PBS. A Leica SP2 confocal system (Leica Microsystems GmbH, Wetzlar, Germany) was used to observe the localization of TTC22V1.

Cell proliferation and migration assays using the IncuCyte platform. CC cell HCT116 and SW480 cells, whose biological behavior was significantly affected by *miR663a* expression changes (13), were seeded into 96-well plates (3,000 cells/well; 6-wells/group) and cultured at 37˚C for at least 96 h to generate proliferation curves. Images were captured of the cells every 2 h. Cell confluence was analyzed with IncuCyte ZOOM software 2015A (Essen Bioscience, Ann Arbor, MI, USA). For the continuous observation of cell migration and invasion, cells were seeded into 96-well plates at a density of 10,000 cells/well and cultured for 24 h. Subsequently, a wound was made in the cell layer, and the cells were washed 3 times with PBS. The cells were regularly cultured and photographed every 2 h for at least 96 h. The relative wound density and the width were calculated using the same software.

Transwell invasion assay. Plates (24-well) with Transwell permeable supports with a 6.5 mm insert and an 8.0 μm polycarbonate membrane (Corning, Inc., Corning, NY, USA) were used in the cell invasion assay. The upper chamber was pre-coated with a 100 μl mixture of BD Matrigel (BD Biosciences, San Jose, CA, USA) and RPMI-1640 (1:5, v/v). The lower chamber contained 800 μl RPMI-1640 medium containing 10% FBS. Cells were seeded into the upper chamber (3,000 cells/well, 3-wells/group). After 24 or 36 h of incubation at 37˚C, the 6.5-mm inserts were removed from the plate, fixed in 4% paraformaldehyde, and stained with a crystal violet solution (0.1%; at room temperature for 30 min). Non-invasive cells on the upper surface of the insert were wiped away with a cotton swab. The number of invaded cells was counted manually in 4 randomly selected fields under a light microscope. All experiments were performed at least 3 times.

Dual-luciferase reporter assay. The wild-type *TTC22V1* 3'UTR was inserted into the pGL-control vector (cat. no. E1741; Promega Corporation, Madison, WI, USA) and used to transfect HCT116 cells in a 24-well plate using X-tremeGENE™ HP DNA transfection reagent (Roche Diagnostics GmbH). Pre-miR663a or the control vector was co-transfected with the *Renilla* vector (3-wells/group). The activities of both *Renilla* and firefly TTC22V1 3'UTR-wt/-mut luciferases were determined using a Dual-Luciferase Reporter Assay system (Promega Corporation) at 72 h post-transfection.

RNA pulldown assay. HCT116 cells ($3x10^6$) seeded in a 10-cm plate for 24 h were transfected with biotin-labeled miR-NC (forward, 5'-uucuccgaacgugucacgutt-3' and reverse, 5'-acgugacacguucggagaatt-3'); biotin-labeled miR663a-wt (forward, 5'-aggcggggcgccgcgggaccgc-3' and reverse, 5'-gcgguccgcgcgccccgccu-3'); or biotin-labeled miR663a-mut (forward, 5'-cuuacauucgccgcgggaccgc-3' and reverse, 5'-gcgguccgcggcgaauguaag-3') (final concentration, 100 nM). The cell lysates were harvested at 48 h. Streptavidin Dynabeads (Dynabeads® M-280 Streptavidin; cat. no. 11205D; Thermo Fisher Scientific, Inc.) (50 μl/pulldown) were coated with 10 μl yeast tRNA (stock, 10 mg/ml; Ambion; Thermo Fisher Scientific, Inc.), 10 μl BSA (10 mg/ml stock) and 480 μl lysis buffer and incubated with rotation at 4˚C for 30 min. The beads were washed and mixed with sample lysates (600 μl/pulldown) and incubated overnight at 4˚C on a rotator. The beads were then

pelleted the next day to remove the unbound materials and were digested with 5 μl RNase-free DNase I (2 U/μl) at 37˚C for 10 min and 5 μl proteinase K (10 mg/ml) at 55˚C for 20 min. Subsequently, together with 50 μl input, RNA was extracted, and RT-qPCR was used to detect the target *TTC22V1* mRNA as aforementioned.

Tumor implantation and experimental metastasis. Non-obese diabetic (NOD)-severe combined immunodeficient (SCID) mice (n=30; female, 6-8 weeks, 18-20 g) were purchased from Beijing HFK Bioscience Co., Ltd. (Beijing, China) and were allowed to acclimatize for 1 week before use. Housing conditions were 25˚C, humidity 45-55%, 1 atm pressure, 12-h light/12-h dark cycle, free choice feeding, water *ad libitum*. Cells stably transfected with the GFP-*miR663a* and control vectors were digested with trypsin. A cell suspension ($1x10^7$ cells/ml) was injected subcutaneously (150 μl/site, 10 mice/group) into the left and right legs of NOD-SCID mice, respectively. At 3 weeks after implantation, the mice were sacrificed and the weights of their xenograft tumors were determined.

To examine experimental metastasis, $1.25x10^6$ HCT116 cells stably transfected with the GFP-*miR663a* or control vector were injected into the tail veins of NOD-SCID mice (10 mice/group). After 2 months, the mice were sacrificed and dissected. Metastatic nodules in the lung and liver surfaces were counted. Tissues were fixed in formalin and prepared to create 4-μm paraffin-embedded slices. The slices were stained with 0.125% hematoxylin and 1% eosin at room temperature for 10 min and observed via light microscopy.

miR663a target selection. The list of possible *miR663a* target candidates was downloaded from the miRNAMap website (mirnamap.mbc.nctu.edu.tw/php/mirna_entry.php?acc=MI0003672) and obtained from the National Center for Biotechnology Information (NCBI) website (blast.ncbi.nlm.nih.gov) through searching the *miR663a* matched mRNA-3'UTRs in the human genome and transcripts. When downregulation (or upregulation) of target gene expression was >1.5-fold in HCT116 cells 72 h after transient transfection of *miR663a* expression vector (or antisense/inhibitor treatment) in the Affymetrix U133 Plus 2.0 cDNA array datasets (NCBI Gene Expression Omnibus accession no. GES117918) (13), it was selected as the candidate target.

Statistical analyses. All statistical analyses were performed using SPSS software (version 18.0; SPSS, Inc., Chicago, IL, USA). The Shapiro-Wilk test was used to estimate the normality of the distributions. Student's t-test or one-way analysis of variance was used for normally distributed data. Patient overall survival times were analyzed using the Kaplan-Meier method and log-rank test. Cox's proportional hazard model was used for multivariate analyses. Differences in *miR663a* and *TTC22V1* expression levels were assessed using the Mann-Whitney U test or Wilcoxon signed-rank test. Spearman's non-parametric analyses were performed to determine the correlation between gene expression. $P<0.05$ was considered to indicate a statistically significant difference. All experiments were performed at least 3 times with samples in triplicate.

Results

Downregulation of miR663a expression in CC tissues. To the best of our knowledge, the expression status of *miR663a* in CC tissues has not been reported previously. Using qPCR analysis, it was identified that the relative *miR663a* expression levels in CC tissues were significantly decreased compared with those in SM tissues from 172 patients (median, 0.263 vs. 0.555; Mann-Whitney U test, P=0.001; Fig. 1A). In addition, the *miR663a* expression levels in metastatic CC tissues were also significantly decreased compared with those in non-metastatic CC tissues (P=0.044; Fig. 1B and Table I). No significant association between *miR663a* expression and age, sex, vascular embolus, CC differentiation and location was identified. The downregulation of *miR663a* expression in CC tissues, particularly in metastatic CC tissues, indicated that *miR663a* may serve an important role in carcinogenesis and metastasis in CC.

Inhibition of cancer cell proliferation and metastasis by miR663a in vitro and in vivo. To investigate the effects of *miR663a* overexpression on CC cell proliferation, migration and invasion, cells were transiently transfected with the pre-*miR663a* expression vector and its control vector pcDNA3.1b. Forced *miR663a* overexpression significantly inhibited proliferation, migration and invasion in HCT116 cells (Fig. 2A and B) and SW480 cells (Fig. 2C and D).

To validate the *in vitro* results, the GFP-*miR663a* vector was used to stably transfect HCT116 cells (Fig. 3A). The growth of HCT116 xenografts (tumors) in NOD-SCID mice was significantly decreased by *miR663a* overexpression (P<0.001; Fig. 3B). GFP-*miR663a* tumors were observed in only 7/10 mice, whereas GFP-Ctrl tumors occurred in 10/10 mice. The *miR663a* expression levels in GFP-*miR663a* tumors were ~2-fold higher compared with those in the GFP-Ctrl tumors (Fig. 3C, left).

An experimental pulmonary metastasis model of NOD-SCID mice was used to determine whether *miR663a* overexpression could inhibit cancer metastasis. At 2 months after injection of HCT116 cells stably overexpressing *miR663a* into the tail veins of mice (*miR663a* group), the average number of metastatic nodules on the lung surfaces in the *miR663a* group was significantly lower compared with in the Ctrl group (median, 1.2 vs. 6.1; Mann-Whitney U test; P=0.0383; Fig. 3D, left). The average lung weight, which correlates positively with the number of metastatic nodules, was also lower in the *miR663a* group compared with in the Ctrl group (median, 0.430 vs. 0.575 g; Mann-Whitney U test; P=0.041; Fig. 3D, right). In addition, metastatic nodules were observed on the lung surfaces of 50% (5/10) of the mice, whereas the lung metastatic rate was 70% (7/10) in mice injected with the cells stably transfected with the control vector (Ctrl group), including 2 giant metastatic lesions on the lung hilus (Fig. 3E, white arrow). These results indicate that *miR663a* overexpression inhibits experimental metastasis in HCT116 cells *in vivo*.

Characterization of TTC22V1 mRNA as a crucial miR663a target. To search for candidate *miR663a* targets in CC tissues, a bioinformatics analysis was performed using sequence search

Table I. Comparison of *miR663a* and *TTC22V1* gene expression level in colon carcinoma with various clinicopathological characteristics.

Characteristics	n	Median relative expression level of *miR663a* (interquartile range)	P-value	Median relative expression level of *TTC22V1* mRNA (interquartile range)	P-value
Age, years			0.286		0.134
≤60	75	0.31 (0.15-0.56)		0.07 (0.03-0.17)	
>60	97	0.25 (0.12-0.47)		0.01 (0.05-0.22)	
Sex			0.295		0.820
Male	101	0.29 (0.15-0.49)		0.08 (0.04-0.17)	
Female	71	0.23 (0.09-0.53)		0.09 (0.03-0.17)	
Location			0.962		0.432
Sigmoid	87	0.30 (0.10-0.51)		0.08 (0.03-0.18)	
Others	85	0.25 (0.14-0.65)		0.08 (0.05-0.21)	
Differentiation			0.065		0.162
Poor	39	0.34 (0.13-0.65)		0.11 (0.03-0.25)	
Moderate/well	133	0.25 (0.11-0.49)		0.07 (0.04-0.15)	
Vascular embolus			0.931		0.076
Negative	140	0.26 (0.11-0.55)		0.07 (0.03-0.16)	
Positive	32	0.28 (0.15-0.47)		0.09 (0.06-0.28)	
pTNM stage			0.047		0.020
I+II	89	0.33 (0.12-0.71)		0.06 (0.03-0.14)	
III+IV	83	0.25 (0.13-0.35)		0.09 (0.04-0.27)	
Depth of invasion			0.443		0.286
T_{1-3}	101	0.25 (0.12-0.51)		0.06 (0.03-0.15)	
T_4	71	0.32 (0.14-0.52)		0.08 (0.04-0.21)	
Lymph metastasis			0.044		0.022
$Negative_0$	88	0.33 (0.12-0.71)		0.06 (0.03-0.14)	
Positive	84	0.25 (0.14-0.35)		0.08 (0.04-0.26)	
Distant metastasis			0.981		0.002
M_0	147	0.27 (0.12-0.52)		0.07 (0.03-0.15)	
M_1	25	0.25 (0.14-0.51)		0.13 (0.07-0.65)	

Statistical significance was determined using a Mann-Whitney U test. *TTC22V1*, tetratricopeptide repeat domain 22 variant 1; pTNM, pathological tumor-node-metastasis.

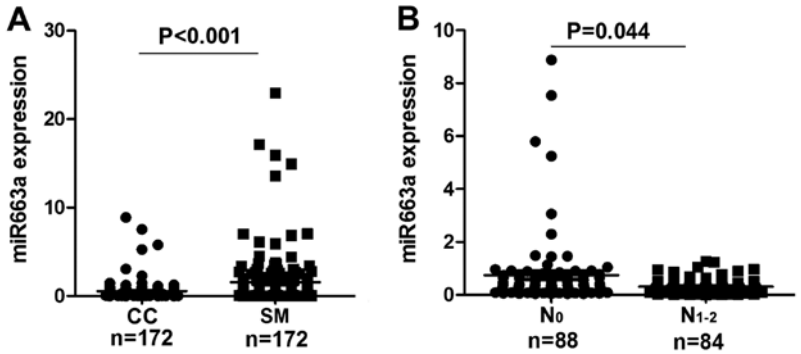

Figure 1. Comparison of *miR663a* expression levels in colon cancer tissue samples using the reverse transcription-quantitative polymerase chain reaction. (A) CC and the corresponding SM samples from 172 patients with CC. (B) CC with or without lymph node metastasis at the time of surgical resection. *miR663a*, microRNA-663a; CC, colon cancer; SM, surgical margin.

strategies. cDNA array datasets (NCBI Gene Expression Omnibus accession no. GES117918) were also used to select *miR663a* target genes in HCT116 cells transiently transfected with the *miR663a* expression vector or its inhibitor/antisense as

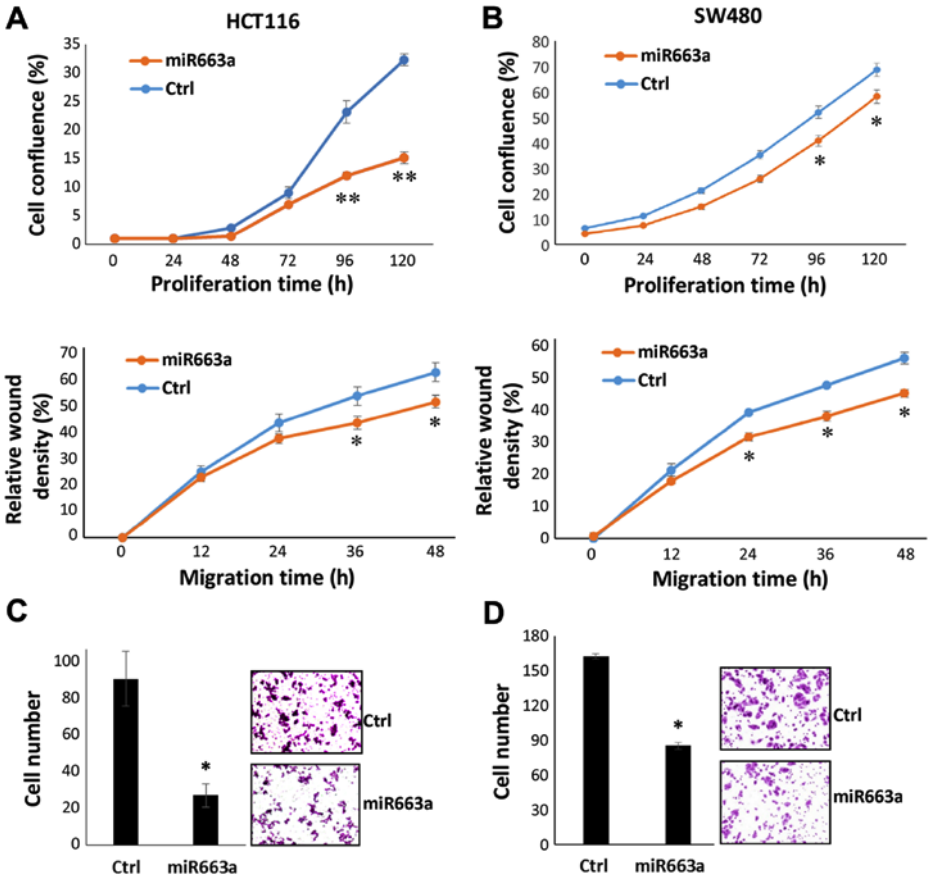

Figure 2. Effects of *miR663a* overexpression on the proliferation, migration and invasion of colon cancer cells. (A) Proliferation and migration curves for HCT116 cells transfected with the pre-*miR663a* vector according to long-term IncuCyte analyses; each point represents the mean ± standard deviation value for 5-wells. (B) Proliferation and migration curves for SW480 cells transfected with the pre-*miR663a* vector according to long-term IncuCyte analyses; each point represents the mean ± standard deviation for 5-wells. (C) Invasion of HCT116 cells transiently transfected with the pre-*miR663a* vector and control vector according to a typical Transwell analysis (triplicate results). (D) Invasion of SW480 cells transiently transfected with the pre-*miR663a* and control vector according to a typical Transwell analysis (triplicate results). *P<0.05; **P<0.01 vs. Ctrl. Ctrl, pcDNA3.1b scrambled RNA control vector; *miR663a*, microRNA-663a.

we reported previously (13). The bioinformatics analysis results indicated that *FAM120A*, *KLF5*, *MBTD1*, *PSMG1*, *RBL1*, *TTC22V1*, *ZMYM5* and *ZNF131* mRNAs may be *miR663a* candidate targets. However, RT-qPCR analysis results revealed that *TTC22V1* mRNA was the only one whose expression level was consistently and inversely altered >1.5-fold following *miR663a* overexpression and knockdown by transient transfection with *miR663a* mimic and inhibitor/antisense in HCT116 cells, respectively (Fig. 4A). *TTC22V1* expression was down-regulated in GFP-*miR663a* tumors (Fig. 3C, right and Fig. S1). Such an association could not be detected for *FAM120A*, *KLF5*, *MBTD1*, *RBL1*, *ZMYM5* or *ZNF131* (Fig. S2). Western blot analyses confirmed these results in HCT116, RKO and MKN45 cells (Fig. 4B). In the dual-luciferase assays, *miR663a* mimic significantly decreased the activity of the wild-type *TTC22V1* 3'UTR reporter (3'UTR-wt; P=0.010), but not that of the 3'UTR-mut, which did not match the 5'-fragment of mature *miR663a* (Fig. 4C). In addition, in an miRNA pull-down assay, *TTC22V1* mRNA interacted with only wild-type *miR663a* and not with the *miR663a* mutant (Fig. 4D).

To determine the roles of *TTC22V1* in the inhibition of the migration and invasion of HCT116 cells by *miR663a*, *TTC22V1*&3'UTR-wt and *TTC22V1*&3'UTR-mut control vectors, integrated with full-length *TTC22V1* cDNA and 3'UTR-wt or 3'UTR-mut control sequences, were specifically constructed and used to transiently transfect HCT116 and SW480 cells. The results of long-term dynamic IncuCyte analyses indicated that *TTC22V1*&3'UTR-wt and *TTC22V1*&3'UTR-mut expression significantly enhanced the migration of the cells (Fig. 5A and B). Notably, *miR663a* mimic transfection significantly decreased the migration of these cells transfected with *TTC22V1*&3'UTR-wt, but only slightly (not significantly) decreased the migration of the cells transfected with *TTC22V1*&3'UTR-mut: 15.90 vs. 4.54% for HCT116 cells at 36 h, and 19.17 vs. 9.18% for SW480 at 60 h (Fig. 5A and B). The typical Transwell assay results revealed similar differences for cell invasion (Fig. 5C and D).

To determine whether the *miR663a-TTC22V1* axis is actually involved in CC prognosis, *TTC22V1* expression levels in 172 CC tissues and the corresponding SM tissues were determined using RT-qPCR. The results indicated that *TTC22V1* mRNA levels were significantly lower in CC tissues compared with in SM tissues (P<0.001; Fig. 6A). Western blot analyses were consistent with the RT-qPCR results (Fig. 6B). Notably, a significant reverse correlation between *miR663a* and *TTC22V1* expression levels was also identified for 172 CC tissues (R=-0.21; P=0.006; Fig. 6C). This result further indicates that TTC22V1 is an *miR663a* target.

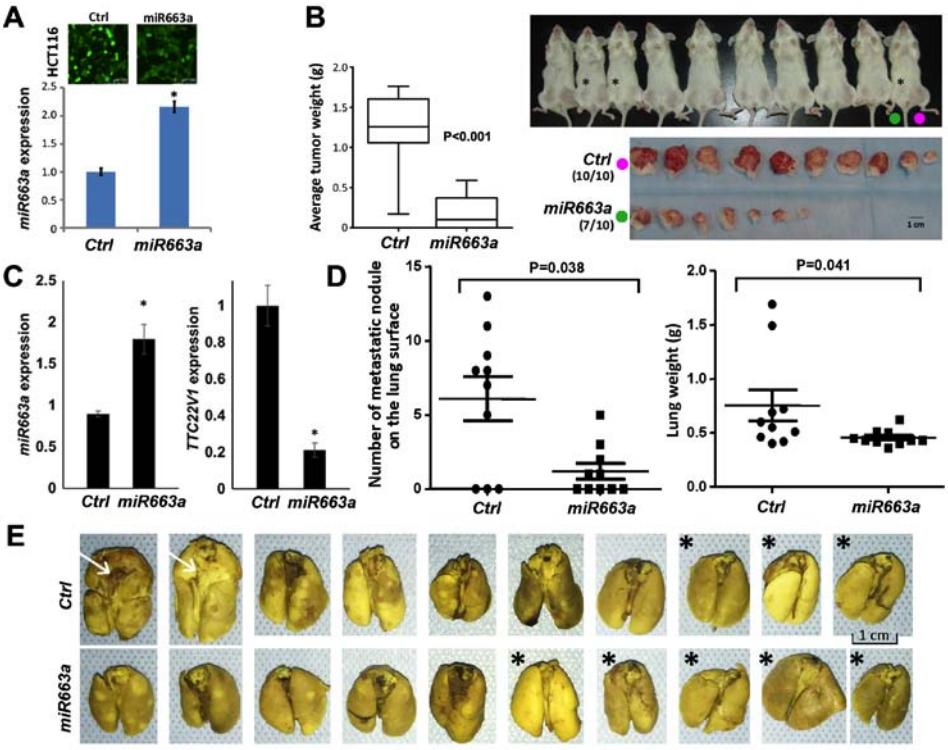

Figure 3. Effects of *miR663a* overexpression on the proliferation and experimental pulmonary metastasis of HCT116 cells in NOD-SCID mice. (A) *miR663a* expression in HCT116 cells stably transfected with the GFP-*miR663a* and control vectors. (B) HCT116 cell proliferation in NOD-SCID mice. Cells stably transfected with GFP-*miR663a* and control vector were injected subcutaneously into the left and right legs of each mouse, respectively. (C) *miR663a* and tetratricopeptide repeat domain 22 variant 1 expression levels in GFP-*miR663a* and GFP-Ctrl tumors determined using reverse transcription-quantitative polymerase chain reaction analysis. *P<0.05 vs. Ctrl. (D) Number of metastatic nodules on the lung surface (left) and the weight of the lungs in the 2 groups of mice (right). (E) Images of the lungs with visible metastasis nodules in the *miR663a* stable overexpression and control groups of mice (Ctrl). The lungs without metastatic nodules are indicated with a star. Two lungs with giant metastatic lesions at the hilus in the Ctrl group are indicated with a white arrow. *miR663a*, microRNA-663a; NOD-SCID, non-obese diabetic-severe combined immunodeficient; GFP, green fluorescent protein; Ctrl, GFP-scrambled RNA control vector.

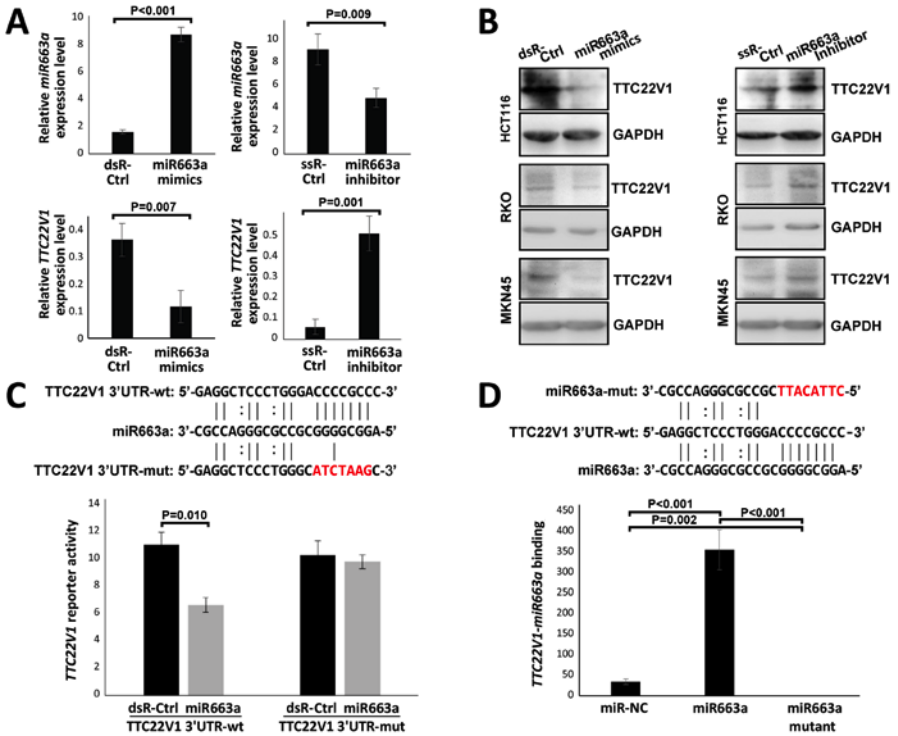

Figure 4. Association between *miR663a* and *TTC22V1* expression levels. (A) Changes in expression levels of *TTC22V1* mRNA in HCT116 cells with forced *miR663a* expression changes determined using reverse transcription-quantitative polymerase chain reaction analyses. (B) Western blot analysis of the amount of TTC22V1 in HCT116, RKO and MKN45 cells transiently transfected with *miR663a* mimic, antisense/inhibitor and negative control. (C) Dual-luciferase assay results of the effect of *miR663a* on the reporter activity of wild-type TTC22V1 3'UTR and its mutant in HCT116 cells. (D) Biotin-labeled *miR663a* pulldown assay results indicating interactions between *TTC22V1* mRNA and *miR663a* or its mutant. *miR663a*, microRNA-663a; *TTC22V1*, tetratricopeptide repeat domain 22 variant 1; UTR, untranslated region; wt, wild-type; mut, mutant; dsR, scrambled short interfering RNA; ssR, scrambled RNA; Ctrl, control.

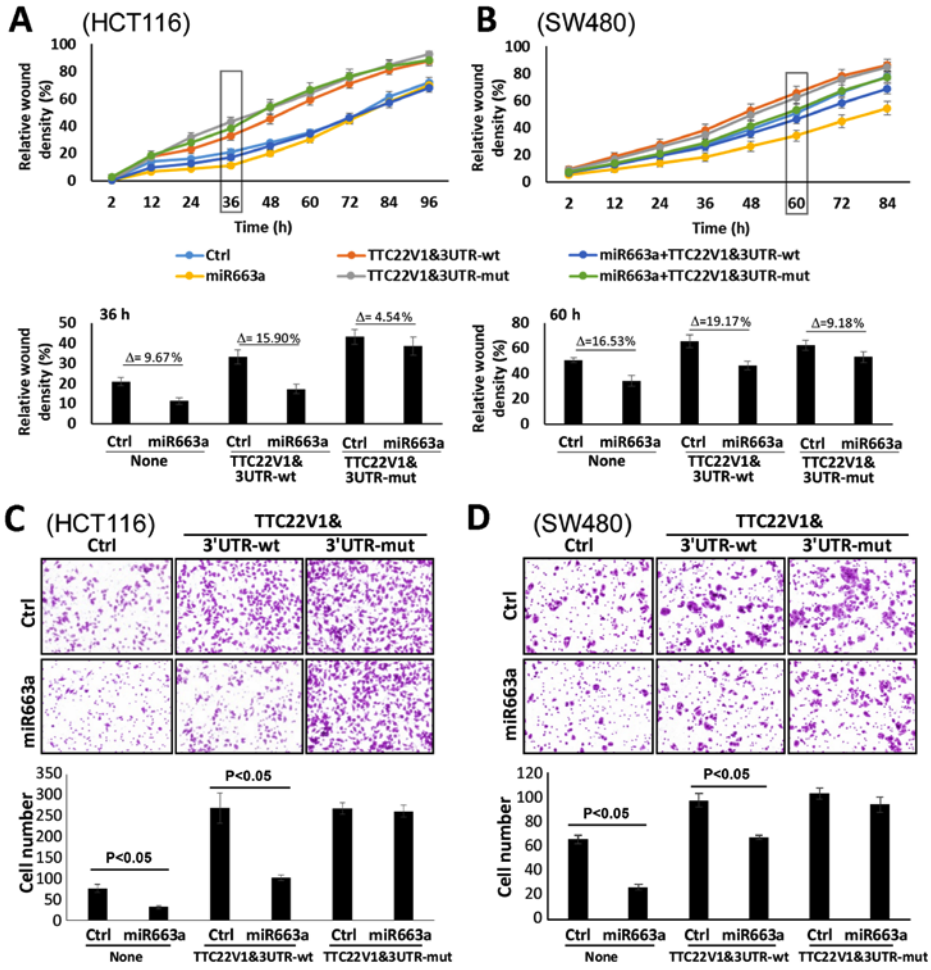

Figure 5. Effects of *miR663a* on the migration and invasion of colon cancer cells transiently transfected with wild-type *TTC22V1* 3'UTR and its mutant control. Migration curves for (A) HCT116 and (B) SW480 cells transiently co-transfected with the *miR663a* expression vector and TTC22V1&3'UTR-wt or TTC22V1&3'UTR-mut determined using long-term IncuCyte analyses. The cell density data for HCT116 cells at 36 h and for SW480 cells at 60 h are presented in the lower histograms. Each point represents the average value of 5-wells. Differences in the wound density between the *miR663a* and control groups of cells with and without TTC22V1&3'UTR-wt/mut transfection are indicated. Typical Transwell analysis results for the invasion of (C) HCT116 and (D) SW480 cells co-transfected with the *miR663a* vector and TTC22V1&3'UTR-wt or TTC22V1&3'UTR-mut plasmids in triplicate. The migration times were 24 h for HCT116 cells and 36 h for SW480 cells. *miR663a*, microRNA-663a; *TTC22V1*, tetratricopeptide repeat domain 22 variant 1; *TTC22V1*&3'UTR-wt, *TTC22V1* cDNA sequence containing a wild-type 3'UTR; *TTC22V1*&3'UTR-mut, *TTC22V1* cDNA sequence containing a 3'UTR mutant; Ctrl, pcDNA3.1b scramble RNA control vector.

IHC staining demonstrated that the TTC22V1 protein was located principally in the nuclei of epithelial cells at the crypt base (or stem cell niche) in the SM mucosa samples (Fig. 6D), but no TTC22V1 staining signals were observed in the CC samples (Fig. 6E). Only weak (if any) cytoplasmic TTC22V1 staining was detected in the CC cells. According to the immunofluorescence confocal microscopy assays, TTC22V1 protein staining signals could be observed in the nuclei and cytoplasm in HCT116 and Caco2 cells, but only in the nucleus in SW480 (Fig. S3). Nuclear speckles enriched with endogenous TTC22 protein were also frequently observed in these cells.

Notably, more *TTC22V1* mRNA was detected in metastatic CC compared with in non-metastatic CC (Mann-Whitney U test; P=0.022 for lymph metastasis and 0.002 for distant metastasis; Table I). According to the Kaplan-Meier survival analysis, the overall survival time was significantly shorter for patients with CC with high *TTC22V1* expression compared with for those with low *TTC22V1* expression (log-rank test; P=0.023; Fig. 6F). High *TTC22V1* expression remained a significant poor survival factor following adjustment for age, sex, location, depth of invasion, differentiation, vascular embolism, lymph metastasis and distant metastasis (adjusted-hazard ratio, 1.765; 95% confidence interval, 1.013-3.076; P=0.045). Collectively, these results suggest that *TTC22V1* may be a metastasis-associated gene and crucial *miR663a* target.

Discussion

Primate-specific *miR663a* is a rare gene located in the sequence flanking the centromere of chromosome 20. It is well-known that *miR663a* is an inflammation-associated miRNA (1-6) and that local chronic inflammation contributes to colorectal cancer (25-29). However, it is unknown whether alterations in *miR663a* expression contribute to CC development and progression. Conflicting results in previous studies suggest that the effects of *miR663a* on cancer development and progression may be tissue/organ-dependent (7-12). In

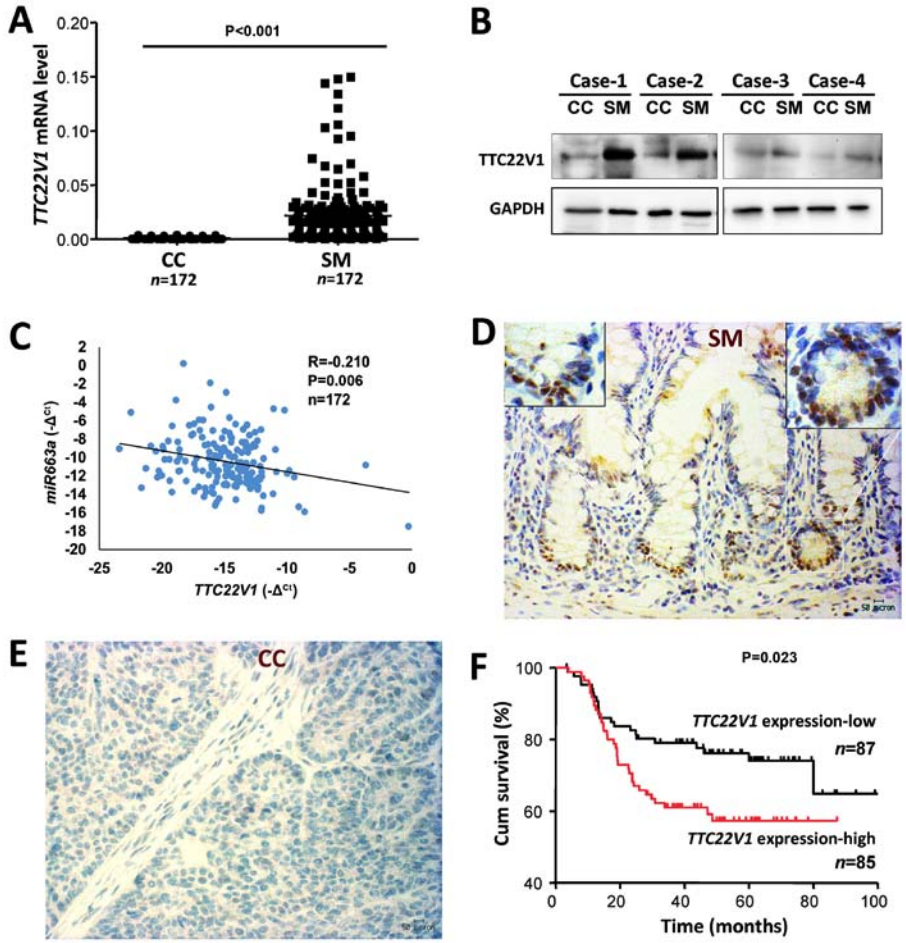

Figure 6. Downregulation of *TTC22V1* expression associated with CC metastasis. (A) Comparison of *TTC22V1* expression levels in CC and paired SM samples using the reverse transcription-quantitative polymerase chain reaction. (B) Comparison of *TTC22V1* expression levels in CC and paired SM samples using western blot analysis. (C) Association between *TTC22V1* and *miR663a* RNA levels in 172 CC tissues using *ALU* and *U6* as reference genes. (D) TTC22V1 staining; 2 crypt bases with nucleic TTC22-positive epithelial cells in representative SM tissues are presented in the insets. (E) No TTC22 staining signals were observed in paired CC tissues. (F) Kaplan-Meier survival curves for patients with CC classified into high and low *TTC22V1* expression groups. The cut-off value to define high *TTC22V1* expression samples was >0.0008. TTC22, tetratricopeptide repeat domain 22; *TTC22V1*, TTC22 variant 1; CC, colon cancer; SM, surgical margin; *miR663a*, microRNA-663a; Cum, cumulative.

the present study, it was identified that *miR663a* expression was downregulated during CC development and that low *miR663a* expression was associated with a high risk of CC metastasis. The *in vitro* and *in vivo* experimental results suggest that *miR663a* is a suppressor of CC progression. Most importantly, it was identified, for the first time, to the best of our knowledge, that *TTC22V1* mRNA is a crucial *miR663a* target in CC cells. *TTC22V1* significantly increased CC cell migration and invasion, and the risk of CC metastasis, and decreased patient survival times. These results indicate that the *miR663a-TTC22V1* axis may serve an important role in CC metastasis.

Currently, there is no information on the biological function of the *TTC22* gene. The bioinformatics analysis of the Cancer Cell Line Encyclopedia data revealed that *TTC22V1* shared the most co-expressed genes with *CDH1* in human cell lines (n=1037; data not shown) (30). According to publicly available transcriptome databases for various human tissues and the Protein Atlas (20,31), *TTC22* is markedly expressed in the gastrointestinal epithelium, female organs and skin, which are frequently exposed to environmental factors. Furthermore, *TTC22V1* expression is extensively downregulated in a number of types of cancer. The IHC analysis of the present study demonstrated further that the TTC22 protein is located principally within the nuclei of epithelial cells at normal colon crypt base stem cell niches and that nucleic TTC22 is lacking in the majority of CC tissues. RT-qPCR and western blot results confirmed considerably lower *TTC22V1* expression in CC tissues compared with in SM tissues. These results imply that TTC22 is involved in maintaining regular epithelium regeneration in the colon mucosa and the intense self-renewal kinetics of intestinal stem cells. Notably, *TTC22V1* mRNA levels were significantly higher in metastatic CC compared with in non-metastatic CC, and forced *TTC22V1* overexpression increased CC cell migration and invasion. The overall survival times of patients with CC with high *TTC22V1* mRNA levels was much shorter compared with that of patients with low *TTC22V1* expression. Similar survival differences were also identified in several public databases of patients with CC (bioinformatica.mty.itesm.mx:8080/Biomatec/SurvivaX.jsp) (32-34) (Fig. S4). These results suggest that *TTC22V1* is required for CC cell migration and subsequent metastasis. It is worthwhile to investigate whether nucleic TTC22V1 is essential for the shift in regener-

ating cells from the base crypt to the mucosa surface and the migration of CC cells.

Generally, the majority of mature miRNAs bind to the target mRNA 3'UTR and 5'UTR in the cytoplasm, leading to target mRNA degradation or translation inhibition. The functions of miRNAs are largely dependent on the expression patterns of target genes in the cells. Except for *TTC22V1*, however, expression changes in other *miR663a* target genes were not detected in HCT116 cells with *miR663a* overexpression or downregulation in the present study. It was also determined that *miR663a* overexpression could significantly inhibit migration and invasion in CC cells overexpressing *TTC22V1* containing the 3'UTR-wt sequence, but only slightly inhibit migration and invasion in cells overexpressing the 3'UTR-mut counterpart. These results provide direct evidence to support *TTC22V1* being a crucial factor for inhibiting the migration and invasion of CC cells by *miR663a*.

In conclusion, the results of the present study revealed that *TTC22V1* mRNA is a crucial *miR663a* target. Whereas *miR663a* suppresses CC metastasis, *TTC22V1* promotes CC metastasis. The *miR663a-TTC22V1* axis may serve an important role in CC metastasis and thus be a target for preventing CC progression.

Acknowledgements

The authors thank Dr Xin Bi from the University of Pennsylvania (Philadelphia, PA, USA) for her writing assistance.

Funding

The present study was supported by the National Natural Science Foundation of China (grant no. 81372592).

Availability of data and materials

The datasets used during the present study are available from the corresponding author upon reasonable request.

Authors' contributions

WT, YD, YM and BZ analyzed gene interactions, and interpreted the patient data regarding gene expression and colon cancer prognosis. LG and JZ participated in the collection of cancer tissues and determination of gene expression levels. WT, YD and DD designed these experiments and were major contributors to writing the manuscript. DD conceived the idea for the study and supervised the entire project. All authors read and approved the final manuscript.

Ethics approval and consent to participate

The Peking University Cancer Hospital and Institutional Review Boards approved this study. All patients provided written informed consent to participate in the study. Ethical approval for the animal experiments was obtained.

Patient consent for publication

Not applicable.

Competing interests

The authors declare that they have no competing interests.

References

1. Dreher A, Rossing M, Kaczkowski B, Nielsen FC and Norrild B: Differential expression of cellular microRNAs in HPV-11 transfected cells. An analysis by three different array platforms and qRT-PCR. Biochem Biophys Res Commun 403: 357-362, 2010.
2. Liang P, Lv C, Jiang B, Long X, Zhang P, Zhang M, Xie T and Huang X: MicroRNA profiling in denatured dermis of deep burn patients. Burns 38: 534-540, 2012.
3. Li P, Zhu N, Yi B, Wang N, Chen M, You X, Zhao X, Solomides CC, Qin Y and Sun J: MicroRNA-663 regulates human vascular smooth muscle cell phenotypic switch and vascular neointimal formation. Circ Res 113: 1117-1127, 2013.
4. Miao CG, Shi WJ, Xiong YY, Yu H, Zhang XL, Qin MS, Du CL, Song TW, Zhang B and Li J: MicroRNA-663 activates the canonical Wnt signaling through the adenomatous polyposis coli suppression. Immunol Lett 166: 45-54, 2015.
5. Hu W, Xu S, Yao B, Hong M, Wu X, Pei H, Chang L, Ding N, Gao X, Ye C, *et al*: MiR-663 inhibits radiation-induced bystander effects by targeting *TGFB1* in a feedback mode. RNA Biol 11: 1189-1198, 2014.
6. Latruffe N, Lançon A, Frazzi R, Aires V, Delmas D, Michaille JJ, Djouadi F, Bastin J and Cherkaoui-Malki M: Exploring new ways of regulation by resveratrol involving miRNAs, with emphasis on inflammation. Ann NY Acad Sci 1348: 97-106, 2015.
7. Jiao L, Deng Z, Xu C, Yu Y, Li Y, Yang C, Chen J, Liu Z, Huang G, Li LC, *et al*: miR-663 induces castration-resistant prostate cancer transformation and predicts clinical recurrence. J Cell Physiol 229: 834-844, 2014.
8. Yi C, Wang Q, Wang L, Huang Y, Li L, Liu L, Zhou X, Xie G, Kang T, Wang H, *et al*: MiR-663, a microRNA targeting $p21^{WAF1/CIP1}$, promotes the proliferation and tumorigenesis of nasopharyngeal carcinoma. Oncogene 31: 4421-4433, 2012.
9. Liang S, Zhang N, Deng Y, Chen L, Zhang Y, Zheng Z, Luo W, Lv Z, Li S and Xu T: miR-663 promotes NPC cell proliferation by directly targeting CDKN2A. Mol Med Rep 16: 4863-4870, 2017.
10. Shi Y, Chen C, Yu SZ, Liu Q, Rao J, Zhang HR, Xiao HL, Fu TW, Long H, He ZC, *et al*: miR-663 suppresses oncogenic function of *CXCR4* in glioblastoma. Clin Cancer Res 21: 4004-4013, 2015.
11. Li Q, Cheng Q, Chen Z, Peng R, Chen R, Ma Z, Wan X, Liu J, Meng M, Peng Z, *et al*: MicroRNA-663 inhibits the proliferation, migration and invasion of glioblastoma cells via targeting TGF-β1. Oncol Rep 35: 1125-1134, 2016.
12. Zang W, Wang Y, Wang T, Du Y, Chen X, Li M and Zhao G: miR-663 attenuates tumor growth and invasiveness by targeting eEF1A2 in pancreatic cancer. Mol Cancer 14: 37, 2015.
13. Tian W, Du Y, Ma Y, Gu L, Zhou J and Deng D: *MALAT1-miR663a* negative feedback loop in colon cancer cell functions through direct miRNA-lncRNA binding. Cell Death Dis 9: 857, 2018.
14. Huang W, Li J, Guo X, Zhao Y and Yuan X: miR-663a inhibits hepatocellular carcinoma cell proliferation and invasion by targeting HMGA2. Biomed Pharmacother 81: 431-438, 2016.
15. Afonyushkin T, Oskolkova OV and Bochkov VN: Permissive role of miR-663 in induction of VEGF and activation of the ATF4 branch of unfolded protein response in endothelial cells by oxidized phospholipids. Atherosclerosis 225: 50-55, 2012.
16. Tili E, Michaille JJ, Adair B, Alder H, Limagne E, Taccioli C, Ferracin M, Delmas D, Latruffe N and Croce CM: Resveratrol decreases the levels of miR-155 by upregulating miR-663, a microRNA targeting *JunB* and *JunD*. Carcinogenesis 31: 1561-1566, 2010.
17. Acevedo N, Reinius LE, Vitezic M, Fortino V, Söderhäll C, Honkanen H, Veijola R, Simell O, Toppari J, Ilonen J, *et al*: Age-associated DNA methylation changes in immune genes, histone modifiers and chromatin remodeling factors within 5 years after birth in human blood leukocytes. Clin Epigenetics 7: 34, 2015.
18. Allan RK and Ratajczak T: Versatile TPR domains accommodate different modes of target protein recognition and function. Cell Stress Chaperones 16: 353-367, 2011.
19. Blatch GL and Lässle M: The tetratricopeptide repeat: A structural motif mediating protein-protein interactions. BioEssays 21: 932-939, 1999.

20. Uhlén M, Fagerberg L, Hallström BM, Lindskog C, Oksvold P, Mardinoglu A, Sivertsson Å, Kampf C, Sjöstedt E, Asplund A, *et al*: Proteomics. Tissue-based map of the human proteome. Science 347: 1260419, 2015.
21. Sobin LH and Wittekind Ch (eds): International Union Against Cancer (UICC): TNM classification of malignant tumors. 6th edition. Wiley, New York, 2002.
22. Marullo M, Zuccato C, Mariotti C, Lahiri N, Tabrizi SJ, Di Donato S and Cattaneo E: Expressed Alu repeats as a novel, reliable tool for normalization of real-time quantitative RT-PCR data. Genome Biol 11: R9, 2010.
23. Livak KJ and Schmittgen TD: Analysis of relative gene expression data using real-time quantitative PCR and the $2^{-\Delta\Delta CT}$ method. Methods 25: 402-408, 2001.
24. Tian W, Qu L, Meng L, Liu C, Wu J and Shou C: Phosphatase of regenerating liver-3 directly interacts with integrin β1 and regulates its phosphorylation at tyrosine 783. BMC Biochem 13: 22, 2012.
25. Ullman TA and Itzkowitz SH: Intestinal inflammation and cancer. Gastroenterology 140: 1807-1816, 2011.
26. Liu L, Nishihara R, Qian ZR, Tabung FK, Nevo D, Zhang X, Song M, Cao Y, Mima K, Masugi Y, *et al*: Association between inflammatory diet pattern and risk of colorectal carcinoma subtypes classified by immune responses to tumor. Gastroenterology 153: 1517-1530.e14, 2017.
27. Shivappa N, Godos J, Hébert JR, Wirth MD, Piuri G, Speciani AF and Grosso G: Dietary inflammatory index and colorectal cancer risk - a meta-analysis. Nutrients 9: 9, 2017.
28. Pastille E, Frede A, McSorley HJ, Gräb J, Adamczyk A, Kollenda S, Hansen W, Epple M, Buer J, Maizels RM, *et al*: Intestinal helminth infection drives carcinogenesis in colitis-associated colon cancer. PLoS Pathog 13: e1006649, 2017.
29. Biswas S, Davis H, Irshad S, Sandberg T, Worthley D and Leedham S: Microenvironmental control of stem cell fate in intestinal homeostasis and disease. J Pathol 237: 135-145, 2015.
30. Consortium CCLE; Cancer Cell Line Encyclopedia Consortium; Genomics of Drug Sensitivity in Cancer Consortium: Pharmacogenomic agreement between two cancer cell line data sets. Nature 528: 84-87, 2015.
31. Uhlen M, Zhang C, Lee S, Sjöstedt E, Fagerberg L, Bidkhori G, Benfeitas R, Arif M, Liu Z, Edfors F, *et al*: A pathology atlas of the human cancer transcriptome. Science 357: 357, 2017.
32. Aguirre-Gamboa R, Gomez-Rueda H, Martínez-Ledesma E, Martínez-Torteya A, Chacolla-Huaringa R, Rodriguez-Barrientos A, Tamez-Peña JG and Treviño V: SurvExpress: An online biomarker validation tool and database for cancer gene expression data using survival analysis. PLoS One 8: e74250, 2013.
33. Loboda A, Nebozhyn MV, Watters JW, Buser CA, Shaw PM, Huang PS, Van't Veer L, Tollenaar RA, Jackson DB, Agrawal D, *et al*: EMT is the dominant program in human colon cancer. BMC Med Genomics 4: 9, 2011.
34. Sveen A, Agesen TH, Nesbakken A, Rognum TO, Lothe RA and Skotheim RI: Transcriptome instability in colorectal cancer identified by exon microarray analyses: Associations with splicing factor expression levels and patient survival. Genome Med 3: 32, 2011.